HHS Public Access

Author manuscript

Cell Rep. Author manuscript; available in PMC 2016 April 28.

Published in final edited form as:

Cell Rep. 2015 April 28; 11(4): 539–550. doi:10.1016/j.celrep.2015.03.047.

Cleavage-independent HIV-1 Env trimers engineered as soluble native spike mimetics for vaccine design

Shailendra Kumar Sharma[1], **Natalia de Val**[3], **Shridhar Bale**[2], **Javier Guenaga**[1], **Karen Tran**[1], **Yu Feng**[1], **Viktoriya Dubrovskaya**[2], **Andrew B. Ward**[1,3,4], and **Richard T. Wyatt**[1,2,4,*]

[1]IAVI Neutralizing Antibody Center at The Scripps Research Institute, La Jolla, CA 92037

[2]Department of Immunology and Microbial Science, The Scripps Research Institute, La Jolla, CA 92037

[3]Department of Integrative Structural and Computational Biology, The Scripps Research Institute, La Jolla, CA 92037

[4]Center for HIV/ AIDS Vaccine Immunology and Immunogen Discovery, The Scripps Research Institute, La Jolla, CA 92037

Summary

Viral glycoproteins mediate entry by pH-activated or receptor-engaged activation and exist in metastable pre-fusogenic states that may be stabilized by directed rational design. As recently reported, the conformationally fixed HIV-1 envelope glycoprotein (Env) trimers in the pre-fusion state (SOSIP) display molecular homogeneity and structural integrity at relatively high levels of resolution. However, the SOSIPs necessitate full Env precursor cleavage, which requires endogenous furin over-expression. Here, we developed an alternative strategy using flexible peptide covalent linkage of Env subdomains to produce soluble, homogeneous and cleavage-independent Env mimics, called native flexibly linked (NFL) trimers, as vaccine candidates. This simplified design avoids the need for furin co-expression and, in one case, antibody affinity purification to accelerate trimer scale-up for preclinical and clinical applications. We have successfully translated the NFL design to multiple HIV-1 subtypes, establishing the potential to become a general method of producing native-like, well-ordered Env trimers for HIV-1 or other viruses.

* Corresponding author information: wyatt@scripps.edu, phone; 858 784 7676.

Author Contributions

S.K.S., A.B.W., and R.T.W. designed research; S.K.S., N.d.V., S.B., Y.F., V.D. performed experiments; S.K.S., N.d.V., S.B., J.G., Y.F., K.T., A.B.W, and R.T.W analyzed the data; K.T., A.B.W., and R.T.W wrote the paper.

Accession Numbers

The following EM reconstructions have been deposited in the Electron Microscopy Data Bank: unliganded JRFL gp140 NFL2P (EMD-6293), unliganded BG505 gp140 NFL2P (EMD-6294), JRFL gp140 NFL2P + PGV04 (EMD-6295), BG505 gp140 NFL2P + PGV04 (EMD-6296), JRFL gp140 NFL2P + 2G12 (EMD-6297), BG505 gp140 NFL2P + 2G12 (EMD-6298).

Introduction

The HIV-1 surface unit envelope glycoprotein (Env) trimer is comprised of the heterodimeric gp120 and gp41 subunits, which are the cleavage products of the trimeric Env precursor, gp160. The gp160 is cleaved by the endopeptidase furin in the Golgi complex of Env-expressing host cells (Checkley et al., 2011). Precursor cleavage is necessary for quaternary folding of the noncovalently associated gp120-gp41 subunits, affects the native conformation of the spike, restricts access of non-neutralizing antibodies (non-NAbs) and is required for viral entry into host cells (Herrera et al., 2005; McCune et al., 1988; Pancera and Wyatt, 2005; Ringe et al., 2013).

Numerous studies demonstrate approximately 10-20% HIV-1-infected individuals generate broadly neutralizing antibodies (bNAbs) directed to Env (Stamatatos et al., 2009). The recent isolation of numerous bNAbs from HIV-1 infected individuals shows that, under the right circumstances, the human immune system can generate broadly effective antibodies. The biochemical and structural studies of these bNAbs yields insights about their cognate neutralizing determinants on Env and provides rationale for epitope-specific vaccine targeting. The bNAbs are directed against several accessible sites on gp120 and gp41, including the CD4 binding site (CD4bs), V1/V2 region glycans, glycans at the base of V3, and the gp41 membrane-proximal region (MPER) (West et al., 2014). Recently, other Env sites of vulnerability recognized by bNAbs which span both gp120 and gp41 subunits and involve N-linked glycans are described (Blattner et al., 2014; Falkowska et al., 2014; Huang et al., 2014; Scharf et al., 2014). Many of these bNAbs preferentially recognize Env trimers and are very useful probes for trimer design approaches, such as the one described here.

To generate soluble, stable Env trimers designed to elicit neutralizing antibodies, gp140 oligomers were designed (Forsell et al., 2009). Generally, the gp140s are soluble versions of Env in which the cytoplasmic tail and transmembrane regions of gp41 are deleted, containing full-length gp120 and most of the gp41 ectodomain. The natural association between gp120 and gp41 in the functional Env spike is non-covalent and labile, thereby recombinant expression of cleaved gp140s results in dissociation of the hetero-dimeric subunits. To address this problem, one approach alters the furin cleavage site to covalently link gp120 and gp41, preventing dissociation. Frequently, a trimeric motif (e.g., foldon) is attached at the C-terminus of gp41 to generate uncleaved, stable and soluble gp140 trimers; however, these trimers do not form well-ordered Env spike mimetics (Ringe et al., 2013; Tran et al., 2014). A second strategy introduces a disulfide linkage between gp120 and gp41 by genetically engineering cysteines at the interface of these subunits. The resulting covalently linked gp140s retain the natural cleavage site and are termed “SOS” soluble Env molecules (Binley et al., 2000). An additional HR1 helix destabilizing mutation in the gp41 ectodomain (i.e., I559P, now called SOSIP) greatly improves trimer formation (Sanders et al., 2002) and led to the recent atomic-level structural definition of BG505 SOSIP.664 (Julien et al., 2013; Lyumkis et al., 2013; Pancera et al., 2014; Sanders et al., 2013), hereafter referred to as BG505 SOSIP.

Studies of both cell-surface Env and the soluble SOSIP trimers demonstrate that cleavage is important for native conformation based upon antigenic profiling and EM structural analysis

(Pancera and Wyatt, 2005; Ringe et al., 2013). In these cases, only cleaved trimers preferentially present neutralizing determinants over non-neutralizing and form well-ordered trimers. In contrast, the uncleaved gp140 trimers (e.g. gp140-foldon) generally present selected broadly neutralizing determinants but also present a variety of non-neutralizing epitopes, decreasing their desirability for rational vaccine designs aimed at presenting only neutralizing determinants to the humoral immune system. In the present study, we report a different strategy to generate native-like soluble, but uncleaved or "cleavage-independent", gp140 trimers. We hypothesized that the cleaved termini of gp120 and gp41 are in relatively close proximity and reasoned that covalent linkage of gp120 to gp41 using flexible linkers of specific lengths might allow sufficient conformational mobility for the usually cleaved termini of gp120 and gp41 to orient in a close-to-native, cleaved conformation, resulting in an "uncleaved" but native-like Env trimer.

We employed such a linker strategy to successfully engineer soluble, native-like, cleavage-independent gp140 trimers, termed "Native Flexibly Linked" (NFL) trimers. We used a glycine-serine based (G_4S) flexible peptide linker to replace the furin cleavage motif "REKR" at the natural gp120 C-terminus to achieve covalent linkage to gp41, but allow for the natural association of the Env subunits, resulting in native-like cleavage-independent trimers when used in combination with a gp41 helix-destabilizing substitution. By antigenic, biophysical and structural analyses, we show that these linked trimers display properties consistent with native-like HIV Env spikes, demonstrating the potential for the flexible linker "platform" to be translated into multiple Envs to further HIV-1 vaccine development.

Results

Screening of NFL trimer designs by immunoprecipitation using trimer-preferring bNAbs

A schematic representation depicting the details of the NFL trimer design is shown in Figure 1A (top). The simple but elegant design covalently joins the C-terminus of gp120 to the N-terminus of gp41 that are normally noncovalently linked following precursor cleavage by replacing the gp120 terminal furin cleavage motif "REKR" with a flexible linker (G_4S) of varying lengths. The flexible fusion potentially allows the orientation of the gp120 and gp41 termini in a manner achieved in the cleaved and functional HIV-1 spike. A model illustrating the different linker lengths joining gp120 and gp41 within one monomer, in the context of the trimeric spike is shown in Figure 1A (bottom). For JRFL Env NFL design, we also introduced an E168K change to restore recognition by the PG9/PG16 bNAbs and for BG505 Env NFL, we restored the N-glycan at position 332, the central binding determinant of several recently described bNAbs (Kong et al., 2013).

We expressed the Env NFL trimers for immunoprecipitation (IP) screening to detect well-ordered trimers generated from our initial designs, using three distinct sets of monoclonal antibodies (mAbs). The first set was comprised of the CD4bs-directed bNAbs (b12, VRC01 and PGV04). The second set of mAbs included the trimer-preferring bNAbs (VRC06, PGT145, PGT151 and PG9/PG16) that bind to different regions on the native spike requiring proper conformational packing to form their respective epitopes. These antibodies will detect the presence of well-ordered trimers in a mixture or in purified glycoprotein. The third set was composed of non-NAbs, which do not bind to the functional spike. Recognition

by these antibodies is an indication of uncleaved or disordered trimers and includes the gp41-directed, cluster 1 region-specific mAb, F240, and the non-broadly neutralizing CD4bs-directed mAb, F105. These panels of mAbs were used as an IP-based rapid diagnostic to assess the conformation of the uncleaved gp140s analyzed in our current study (Figure 1B-C). Efficient recognition by the trimer-specific/quaternary-dependent antibodies VRC06, PG16, PGT145 and PGT151 is desired, and such recognition would indicate the presence of well-ordered trimers. Furthermore, a lack of recognition by the non-NAbs would predict a low-level of disordered timers in a given mixture of unpurified proteins.

Initially we scanned for the optimal linker length between gp120 and gp41 using stepwise increases of a G_4S gp120-to-gp41 linker in the JRFL Env prototype context. We included the gp41 I559P change in the initial analysis since this enhances SOSIP trimer formation (Sanders et al., 2002). Three JRFL gp140s with I559P containing 1, 2 or 3 copies of the G_4S linker (JRFL gp140 NFL1P, NFL2P and NFL3P) were synthesized and transiently expressed in 293F cells. IPs were performed with the described mAb panels using the Env-containing supernatants. All three NFLP variants were efficiently immunoprecipitated by the b12 and 2G12 bNAbs (Figure 1B), but were also immunoprecipitated by the non-NAbs F105 and F240. For JRFL gp140 NFL1P, we detected relatively light bands with the trimer-preferring bNAbs VRC06, PGT145 and PGT151 but intense bands with the non-trimer requiring bNAbs (b12, 2G12 and VRC01) and the non-NAbs (F240 and F105). These results indicated that the 1x G_4S linker was not of sufficient length to allow the gp120 and gp41 termini to associate into well-ordered trimers. In contrast, for JRFL gp140 NFL2P, relatively intense bands were observed in the VRC06, PGT145, PGT151 and PG9 IP lanes, indicating that the 2x G_4S linker generated a high percentage of well-ordered, yet uncleaved, but covalently linked trimers. For JRFL gp140 NFL3P, we detected trimer-associated bands, but of less intensity than those in the NFL2P samples, indicating that the 2x linker length was superior. To further optimize the linker length, we scanned lengths between 1x G_4S and 3x G_4S in a stepwise manner, adding one amino acid at a time. As shown in Figure S1A, there was increasing recognition by PGT145 and VRC06 while F105 binding decreased as the linker lengthened from 1x G_4S to 2x G_4S. The converse was true as the linker lengthened to 3x G_4S. Taken together, the 2x linker appears best, with a range of ±2 residues. The 2x linker $(G_4S)_2$, minus the four deleted cleavage-site residues (REKR) that are in effect replaced by the four G residues, would bridge an approximate distance of 22 Å [(10 residues x 3.6 Å per residue) – (4 substituted residues x 3.6 Å)] to link gp120 to gp41. This distance requirement is less than the 36 Å spacing between the gp120 to gp41 termini described in the recent high-resolution BG505 SOSIP crystal structure (Pancera et al., 2014), but is consistent with the experimental titration performed here since 6 residues at the gp41 N-terminus are not visible in that structure and could span over 20 Å.

To explore whether the flexible linker approach could generate a higher fraction of well-ordered trimers derived from another Env, we analyzed a similar subtype A, BG505-based design. We selected the BG505 Env since this strain forms native-like trimers in the SOSIP context, generating more well-formed trimers relative to other known Envs (Sanders et al., 2013). Based on the results of the JRFL gp140 NFLPs linker length scan, we analyzed BG505 NFLs with a 2x linker similarly by IP. The BG505 gp140 NFL2P glycoproteins were efficiently immunoprecipitated by the trimer-preferring bNAbs with similar band intensities,

while IPs with the non-NAbs F105 and F240 showed much fainter bands, suggesting the majority of the transiently expressed BG505 gp140 NFL2P glycoprotein forms well-ordered trimers (Figure 1C).

Previous studies established that the Env gp41 I559P mutation enhances formation of JRFL SOS gp140 into trimeric JRFL SOSIP as well as for BG505 SOSIP (Julien et al., 2013; Khayat et al., 2013; Lyumkis et al., 2013; Sanders et al., 2013; Sanders et al., 2002). Accordingly, our initial screen analyzed the importance of the I559P substitution in the NFL context by comparing JRFL and BG505 gp140 NFL2s with and without the gp41 I559P change. Trimer expression was evaluated by IP using a select mAb panel containing the trimer-specific bNAbs (VRC06, PGT145, PGT151, and PG16), the CD4bs-directed bNAb, VRC01, and the non-NAb F105 (Figure S1B). There were stark differences in the IP band intensities in the VRC06, PGT145, PGT151 and PG16 lanes for both the NFL2 versus NFL2P strain-matched comparisons. Without the I559P substitution in either the JRFL or BG505 context, relatively faint bands were detected following IP with the trimer-specific bNAbs, but prominent bands detected with VRC01 and F105. These data suggested sufficient expression of Env gp140 NFL2, but that the percentage of well-ordered trimers in these preparations was relatively limited. Introduction of the 1559P change appeared to substantially increase well-ordered trimer formation in both Env contexts. The band intensities for the trimer-specific bNAbs was comparable to that of VRC01, while the F105 band was reduced or nearly undetectable (Figure S1B), suggesting that the I559P substitution increased the population of well-formed trimers and decreased the fraction of aberrant misfolded trimers.

Purification of JRFL gp140 NFL2P and BG505 gp140 NFL2P trimers

The JRFL and BG505 gp140 NFL2P glycoproteins were first purified over a lectinagarose column followed by size exclusion chromatography (SEC). The glycoproteins eluted from the lectin column were analyzed by SDS-PAGE, revealing a major band of ~140 kD and confirming that the recombinant proteins were fully uncleaved with the expected molecular weight (Figure S1C). The SEC profiles for both JRFL and BG505 gp140 NFL2P displayed three distinct peaks (Figure 2A, left), which we assigned to aggregates, a predominant trimer fraction and a dimer/monomer fraction, by subsequent blue native (BN) gel analysis (Figure 2B). The gel filtration profile of BG505 gp140 NFL2P (Figure 2A, bottom left), displayed a sharper and more uniform trimer peak with less aggregate and monomer/dimer fractions compared to JRFL gp140 NFL2P (Figure 2A, top left).

To confirm the conformational integrity of the SEC-isolated trimers, we performed diagnostic binding with the trimer-sensitive bNAb PGT145 and non-NAb F105 by bio-layer light interferometry (BLI). For JRFL gp140 NFL2P, though the fraction was trimeric and well recognized by PGT145, it was also recognized by F105 (Figure 2C, top), suggesting the trimer population recovered from SEC contained a mixture of different conformations. We therefore performed negative selection using a F105 mAb affinity column. The disordered trimers or dimer/monomer contaminants bound to the F105 column while the well-ordered trimers were recovered in the flow-through as recently described for JRFL SOSIP trimers

(Guenaga et al., 2015). Subsequent SEC, BN gel analysis, and PGT145/F105 binding profiles (Figure 2D-F) confirmed a well-ordered JRFL NFL2P trimer population.

Interestingly, the preliminary binding analysis of the SEC purified BG505 gp140 NFL2P trimers were recognized marginally by F105, but well recognized by PGT145 (Figure 2C, bottom). The recognition pattern indicated that most of the trimer population following SEC represented native-like trimers. To assess the need for negative selection in the BG505 context, we analyzed the SEC purified trimers and those following negative selection by negative stain EM. A noticeable difference can be seen with JRFL gp140 NFL2P (Figure 3A, top), as aberrant trimers are present before F105 negative selection but not after. Conversely, no qualitative difference in the conformation or overall structure of BG505 gp140 NFL2P (Figure 3A, bottom) was observed before and after F105 negative selection, suggesting that nearly 100% of these uncleaved trimers adopt a native-like conformation. Closer evaluation of EM 2D class averages further validated the homogeneity of JRFL gp140 NFL2P after negative selection (Figure 3B, top) and BG505 gp140 NFL2P without negative selection (Figure 3B, bottom), as distinct and uniform three-lobed, propeller-like structures indicative of well-formed trimers are clearly seen. In contrast, a mixture of irregular shapes is seen with open or ill-formed trimers, as was the case for the strain-matched JRFL gp140-foldon trimers, which were analyzed for comparison (Figure S2A). Accordingly, all further analyses of BG505 gp140 NFL2P trimers were done without negative selection, eliminating the need for antibody affinity purification, while increasing the yield of this native-like, cleavage-independent trimer.

Yields from 1 L of cell culture medium were typically ~4.0 mg of lectin purified protein for JRFL gp140 NFL2P and ~6.0 mg for BG505 gp140 NFL2P, with the trimer fraction after SEC representing ~1.7 mg and 2.5-3.0 mg, respectively. After negative selection, ~1.0 mg of homogeneous, well-folded, uncleaved JRFL gp140 NFL2P trimers were obtained. To further expand the NFL platform to another Env, we expressed and successfully purified clade C 16055 gp140 NFL2P trimers, as shown in the before and after F105 negative selection negative stain EM images (Figure S2B) and EM 2D class averages (Figure S2C). Yields were less than 1 mg per liter for this NFL2P trimer.

Thermal stability of JRFL gp140 NFL2P and BG505 gp140 NFL2P trimers

The thermal stability of the two native-like trimers analyzed here was assessed by differential scanning calorimetry (DSC). A single distinct unfolding peak was obtained for both trimers and the thermal denaturation midpoint temperature (T_m) for JRFL gp140 NFL2P is 56.9°C and 67.6°C for BG505 gp140 NFL2P (Figure 3C). In comparison, JRFL SOSIP measured at 58.2°C in accordance with our recently published value at 58.5°C (Guenaga et al., 2015) and BG505 SOSIP, prepared identically as BG505 gp140 NFL2P, measured at 68.0°C, similar to the previously published 68.1°C (Sanders et al., 2013) (Figure 3C). The T_m of the NFL trimers are within about one degree of the SOSIP trimers, attesting to their similar structural integrity. The sharp melting peak of BG505 gp140 NFL2P trimers indicates that these trimers may be more homogenous compared to JRFL gp140 NFL2P and similar to BG505 SOSIP trimers. To further determine the relative stability of the two NFL trimer-types, we assessed the quaternary stability of these trimers

by isothermal titration calorimetry (ITC) using the Fab derived from the bNAb, VRC01, as a conformational probe. Both the enthalpy and entropy following VRC01 Fab interaction with BG505 gp140 NFL2P trimers were substantially lower compared to that of the JRFL gp140 NFL2P trimers, indicating that the BG505 NFLs may be inherently more well-ordered and stable than the JRFL-based trimers (Figures 3D and S2D). Of note, the VRC01:BG505 trimer enthalpy and entropy are considerably lower than that for VRC01:BG505 gp120, which is consistent with analysis of trimer stability in regards to the VRC01 bNAb (Li et al., 2011).

Antigenic profiling of JRFL gp140 and BG505 NFL2P trimers compared to SOSIP trimers

Ideally, trimer mimetics of the native spike should present most epitopes recognized by the bNAbs, but occlude epitopes recognized by non-NAbs as reported for both BG505 and JRFL SOSIP trimers. To characterize the antigenic profile of the NFL2P trimers, both JRFL and BG505 trimers were captured on ELISA plates pre-coated with an anti-His antibody. We detected efficient recognition by the trimer-preferring bNAbs VRC06, PGT145, PGT151 and PG16 and inefficient recognition by the non-NAbs, especially for BG505 gp140 NFL2P trimers (Figure S3A). In agreement with previous analysis of BG505 SOSIP and the inability of b12 to neutralize BG505 virus, b12 did not recognize the BG505 gp140 NFL2P trimers. The b12 bNAb does neutralize JRFL virus and bound to the JRFL gp140 NFL2P trimers.

We next sought to study the binding kinetics of selected bNAbs and non-NAbs with the NFL2P trimers by biolayer light interferometry (BLI, Octet) as well as to perform head-to-head comparisons to strain-matched SOSIP trimers prepared in a similar manner. We used the previously characterized JRFL gp140-foldon trimers as a comparative control. The mAbs were first captured on anti-Fc sensors and the binding kinetics were assessed with the trimers in solution. Accurate on-rates can be determined in this configuration, but due to avidity effects from the trivalent soluble spike mimetics that, in most cases, can cross bind to three mAbs, accurate off-rates and bona fide affinity cannot be determined for mAbs that bind to each protomer in the trimer. However, for the trimer-specific antibodies that bind to the quaternary structure of the trimer apex with a single binding site, affinities can be determined. Additionally, the trimer-specific antibodies PGT145 and PG16 serve as sensitive probes for the proper quaternary spike packing at the trimer apex, already verified for the SOSIP trimers. With these limitations in mind, all the bNAbs used displayed strong interactions for the soluble NFL2P trimers with rapid on-rates (Figures 4, S3B-C, and Table S1). For PGT145 and PG16, which can bind only one site per trimer and are not subject to avidity gain, the determined K_D of JRFL, BG505 and 16055 gp140 NFL2P trimers were of low nanomolar affinity (Figures 4A and S3C and Table S1). In the case of JRFL and BG505 gp140 NFL2P, the values were comparable to values determined for strain-matched SOSIP trimers determined in a head-to-head manner, indicating that the NFL2P trimer apex is well-ordered (see Figure 4). The non-NAbs F105, b6, and GE136 did not efficiently recognize the NFL2P trimers even with potential avidity, emphasizing the preferable antigenic profile of the NFL2P trimers. Only at the highest concentration of Env (i.e. 200 nM) did we observe low levels of binding. Generally, PGT145 showed the strongest interaction with all the NFL2P Envs compared to other bNAbs used here. PGT151 displayed slightly faster off-rates

in comparison to published values for the BG505 and JRFL SOSIP counterparts ((Blattner et al., 2014; Guenaga et al., 2015) and see Figure S3). This may be due to the NFL engineering at the junction of gp120 and gp41, which may sterically inhibit PGT151 interaction (Blattner et al., 2014). The overall antigenic profiling of JRFL and BG505 gp140 NFL2P determined by BLI was consistent with the ELISA data (Figures 4 and S3), indicating that these two Envs in the NFL2P platform display a favorable antigenic profile.

To further confirm the integrity of the V-region cap at the top of the NFL trimers, we performed additional binding kinetics using two recently described trimer-preferring bNAbs, PGDM1400 and VRC26 (Doria-Rose et al., 2014; Sok et al., 2014). PGDM1400 is PGT145-related and recognized both the BG505 and JRFL NFL:SOSIP pairs with very similar affinities (Figure 4B and Table S1). Although VRC26 does not recognize most clade B Envs, including JRFL, it recognized both BG505 gp140 NFL2P and BG505 SOSIP comparably. Taken together, these binding data suggest that the trimer cap is intact on the NFL trimers as it is on the SOSIP trimers.

Analysis of JRFL and BG505 gp140 NFL2P trimers by EM

We obtained 3D reconstructions of the JRFL and BG505 uncleaved trimers in the unliganded state by negative stain EM (Figure 5A). The overall morphology of the unliganded JRFL and BG505 uncleaved trimers at 22 Å and 20 Å resolution, respectively, is similar to the previously described JRFL SOSIP and BG505 SOSIP (Figure 5B). The trimers display three-lobed structures with an overall density that is wider at the top and narrower at the bottom, consistent with the association of three gp120 units at the top and three gp41 units near the bottom (Sanders et al., 2013). We fitted the higher resolution structure of BG505 SOSIP (PDB 3J5M) within the JRFL and BG505 gp140 NFL2P EM reconstructions to demonstrate that no gross differences were observed. A superimposition of the unliganded JRFL and BG505 gp140 NFL2P densities revealed relatively small differences when comparing their surface contours (Figure 5A, right). These differences may in part be due to the low resolution of the reconstructions and/or the lack of cleavage. To assess how the NFL trimers compared to the well-ordered and well-analyzed SOSIP trimers, we performed superimpositions of JRFL and BG505 gp140 NFL2P to their respective SOSIP counterpart. The densities of the strain-matched trimer sets were very similar in overall structural integrity at this level of resolution (Figure 5B, right).

To further assess the structure of the NFL trimers, complexes were made with bNAbs PGV04, 2G12, and PGT151. 3D reconstructions of JRFL and BG505 gp140 NFL2P trimers liganded with PGV04 (Figure 6A) at 17 Å and 22 Å resolution, respectively, were consistent with the structure of BG505 SOSIP bound to PGV04 (PDB 3J5M). For 2G12 complexes, 3D reconstructions were obtained at 23 Å resolution with JRFL and 20 Å resolution with BG505 gp140 NFL2P (Figure 6B). While the reconstructions are similar to each other, the 2G12 Fab is not as well defined as the previously published BG505 SOSIP in complex with 2G12 (Figures S4A and S5) (Murin et al., 2014). This subtle difference is likely the result of flexibility within the uncleaved trimers or perhaps some heterogeneity in the samples. The trimer-preferring PGT151 binds specific N-linked glycans at the interface of four Env subunits, two gp120 and two gp41 protomers (Blattner et al., 2014; Falkowska et al., 2014).

The EM 2D class averages of PGT151 in complex with either JRFL or BG505 gp140 NFL2P trimers revealed mostly one or two Fabs per trimer (Figure S4B). A lower amount of PGT151 bound to the JRFL uncleaved trimers compared to BG505, which may be due to subtle differences in linker orientation or higher internal flexibility in JRFL gp140. Conformational heterogeneity within the sample precluded calculation of a reliable 3D volume. Computed stoichiometries based on EM micrographs for liganded PGV04, 2G12, or PGT151 cleavage-independent trimers are shown in Table S2.

Overall, the structure of the NFL2P trimers is consistent with that of a well-formed mimic of the native spike. As depicted in Figure 7, covalent linkage of gp120 to gp41 by the 2x linker likely requires the linker to circumvent the neighboring gp41 HR2 helix to span gp120 to gp41 on the same protomer and to achieve near native-like gp120 to gp41 association. We connected gp120 to gp41 with a theoretical linker and a possible path by visual inspection. The distance between the termini calculated from the high resolution BG505 SOSIP structure is ~36 Å; however, the empirically determined best linker length was ~22 Å. This differential may be due to the distance spanned by the six residues not resolved at the gp41 N-terminus in the Pancera BG505 SOSIP structure (ID). We then assessed how this estimated linker path would appear on the gp41 EM density surface at the current level of resolution and observed that this theoretical linker assignment fit well with the EM contours in this “pinwheel-twisted” region of gp41 observable on the “bottom” of the JRFL gp140 NFL2P trimer 3D density (see Figure 7).

Discussion

The NFL design described here represents a simple and potentially more broadly applicable platform to produce cleavage-independent soluble trimers. Consistent with this assertion, respiratory syncytial virus (RSV) fusion (F) protein trimers were recently generated in their pre-fusogenic state using a similar linker strategy, indicating that such an approach might be useful for HIV and other viral glycoproteins (McLellan et al., 2013). One previous attempt using a different linker composition, position, and design objective than our NFL strategy had yielded a completely monomeric Env population (Chow et al., 2002), indicating that the design approach used here are both innovative and critical for the successful generation of well-ordered trimers. We demonstrate that the NFL2P design results in uncleaved but well-ordered trimers, and these stable trimers are antigenically and structurally similar to the BG505 SOSIP trimers. However, the NFL trimers possess an advantage over BG505 SOSIP trimers in that they are cleavage-independent and do not require exogenous furin, which may augment scale up production. We were successful in producing NFL2P trimers from each of subtypes A, B and C, indicating that the flexible linker technology can be translated to multiple Envs and may potentially be more broadly applicable than the SOSIP substitutions.

Cleavage of the gp160 precursor to generate gp120 and gp41 occurs after trimerization in the Golgi, implying that some fraction of the uncleaved trimer population is well-ordered prior to cleavage. A large impact on Env conformation is also imparted after cleavage, indicating that the linker likely allows the gp120 C-terminus and gp41 N-terminus, which are normally liberated by cleavage, to assume their near native-like positions and

orientations. High-resolution of these positions and associations are of interest to further define the structure of the elusive native HIV spike.

We optimized the flexible linker lengths for JRFL and BG505 Envs to 2x G_4S, and both binding and EM analyses with trimer-specific bNAbs indicated that though the linker technology is simple, it is powerfully elegant. In contrast to the assertion that uncleaved trimers do not resemble cleaved, native spikes, we demonstrate that fully uncleaved trimers display an antigenic profile very similar to the cleaved BG505 SOSIP trimers and is consistent with that of the native spike. In the case of JRFL gp140 NFL2P trimers, negative selection was used to eliminate misfolded trimers from the trimer peak cut fraction, revealing ~100% native-like trimers, confirmed by subsequent analyses. Interestingly, for BG505 gp140 NFL2P, the SEC-purified trimer fraction of the lectin-eluted sample showed a favorable antigenic and EM profile with nearly 100% well-ordered trimers, thereby eliminating the need for antibody affinity purification or negative selection. As such, an increased yield of these BG505 native-like trimers can be obtained compared to JRFL. The results also indicate that the increased homogeneity in the well-folded trimeric population of BG505 gp140 NFL2P compared to JRFL is an inherent property of the BG505 primary sequence. Other Envs that resemble BG505 in this property are therefore of high interest.

From the antibody binding studies, the trimer-specific bNAb, PGT151, showed efficient recognition of the JRFL and BG505 gp140 NFL2P glycoproteins though this recognition was not as efficient as that displayed by PGT145. This is perhaps due to a more rapid off-rate as observed by BLI, or perhaps due to the presence of the linker in the region where PGT151 binds to the trimer (Blattner et al., 2014). We did not achieve high occupancy with PGT151 Fab as determined by EM, likely due to direct steric hindrance at the gp120-gp41 junction with the presence of the linker or perhaps due to indirect effects on glycosylation or gp41-related, NFL-specific conformations.

In sum, we demonstrate that cleavage per se is not essential to generate well-folded, native-like HIV-1 Env trimers in the context of an extended linker region. The cleavage-independent JRFL and BG505 gp140 NFL2P Envs are highly homogenous, and may be more amenable to large-scale production. Since exogenous furin is not required, NFL2P trimers may allow a simplified manufacturing pathway in producing GMP-certified cell lines and clinical material. The relatively simple design of the NFL trimer engineering displays the potential to become a general method for producing native-like trimers derived from multiple HIV Envs within a given viral lineage or from different subtypes. On the basis of the data presented here, we believe that the NFL trimer design is a simple and solid foundation to build upon for the overall HIV-1 vaccine development effort. A critical next step is to assess the immunogenicity of the NFL trimers derived from different subtypes compared head-to-head with other strain-matched trimeric Env-based vaccine candidates.

Experimental Procedures

Design of NFL trimer constructs

The JRFL and BG505 primary sequences were modified as follows to express covalently linked soluble gp140s. The native signal sequence was replaced by the CD5 leader and the

MPER was deleted for better expression. The furin cleavage motif at the gp120 C-terminus, "REKR", was deleted and replaced with 1, 2 or 3 copies of the G_4S (GGGGS) flexible linker, joining gp120 covalently to the N-terminus of gp41. The gp140 sequence ends at D664 followed by a G_4S linker, His_8 tag and stop codon. For JRFL, a E168K mutation restores PG9/PG16 binding, and in BG505 T332N restores the N-glycan at position 332. The gene constructs were codon optimized for mammalian expression and synthesized (GenScript). The gp140s designed here are designated as "Native Flexibly Linked" (NFL) Envs, with 1x G_4S named as NFL1, 2x G_4S as NFL2 and 3x G_4S as NFL3. Those containing the I559P mutation were named NFL1P, NFL2P, and NFL3P, respectively.

Expression and purification of the NFL trimers

The NFL Envs were transiently expressed in 293F cells using 293fectin (Invitrogen). Culture supernatants were harvested 4-5 days post transfection and the proteins purified by affinity chromatography using *Galanthus nivalis* lectin-agarose (Vector Labs). The bound protein was eluted with PBS containing 500 mM NaCl and 500 mM methyl-α-D-mannopyranoside and purified by size exclusion chromatography (SEC) using a Superdex 200 10/300 GL column to isolate the total trimer fraction. The trimer peak was either analyzed directly (in the case of BG505 gp140 NFL2P) or subjected to negative selection by F105 antibody affinity columns (in the case of JRFL and 16055 gp140 NFL2P) as previously described (Guenaga et al., 2015). JRFL and BG505 SOSIPs were purified similarly. Samples were analyzed by SDS-PAGE and blue native (BN) gel after each purification step.

Immunoprecipitations

One ml of crude 293F cell supernatant expressing selected NFL and NFLP constructs were incubated with 5 μg of selected mAbs with rocking. Protein A agarose (25 μl) was added to each tube and further incubated to adsorb Env:mAb complexes to the solid phase. After washing three times with PBS containing 500 mM NaCl, the pelleted beads were resuspended in SDS-PAGE loading dye containing 50 mM DTT and boiled prior to SDS-PAGE analysis.

Differential scanning calorimetry

The thermal melting of JRFL and BG505 trimers was analyzed by differential scanning calorimetry (DSC) using a N-DSC II (Calorimety Sciences Corp.). Prior to the DSC scanning, the proteins were dialyzed in PBS, pH 7.4 and concentrated to 0.5 mg/ml. Dialysis buffer was used as the reference solution. The DSC scanning rate was 1°C/min under 3.0 atmospheres of pressure. Data were analyzed after buffer correction, normalization and baseline subtraction using CpCalc software.

Isothermal titration calorimetry

Isothermal titration calorimetry (ITC) measurements were performed using the ITC200 microcalorimeter system (MicroCal Inc.) at 37°C as previously described (Wu et al., 2010). Molar concentrations of gp140 NFL2Ps or gp120s was approximately 3 μM and that of

VRC01 Fab was approximately 80 μM. Data was analyzed with Microcal ORIGIN software using a single-site binding model.

Binding analysis by ELISAs and biolayer light interferometry

ELISA plates coated with 2 μg/ml anti-His mAb were used to capture NFL2P trimers (2 μg/ml) followed by primary mAbs (serially diluted 1:5, starting at 20 μg/ml) and a peroxidaseconjugated goat anti-human secondary Ab (1:10,000). Plates were developed using 3,3', 5,5;-tetramethylbenzidine chromagen solution.

An Octet Red instrument (ForteBio, Pall Life Sciences) was used to study the binding of selected mAbs with the NFL2P trimers by biolayer light interferometry (BLI). In brief, anti-human Fc sensors captured the desired mAbs (5 μg/ml in PBS, pH 7.4). Following a wash in PBS to remove unbound mAbs and establish a baseline, the mAb-loaded sensors were dipped in wells containing two-fold serially diluted trimers (starting at 200 nM) to assess binding. Sensors were then dipped in PBS to obtain the dissociation phase curve. All above operations were done at a shaking speed of 1000 rpm. Data Analysis 7.1 evaluation software (ForteBio) was used to assess the response curves and calculate kinetic parameters using a global fit 1:1 model for applicable mAbs.

Electron microscopy and image reconstruction

JRFL and BG505 gp140 NFL2P trimers were incubated with a ten molar excess of selected Fabs at RT for 1 h. Complexes analyzed included: 1. JRFL with PGV04, 2. JRFL with 2G12, 3. JRFL with PGT151, 4. BG505 with PGV04, 5. BG505 with 2G12 and, 6. BG505 with PGT151. The complexes were applied onto a glow discharged carbon coated 400 Cu mesh grid and negatively stained with 2% uranyl formate for 30 s. Data were collected using a FEI Tecnai Spirit electron microscope and images were acquired with a Tietz 4k X 4k TemCam-F416 CMOS camera at 10° tilt increments, up to 50°.

Fabs were visualized in the 2D class averages if they are bound to the trimer, allowing the percentage of bound trimers relative to unbound trimers to be tabulated. EMAN (Ludtke et al., 1999) was used for all 3D reconstructions. Resolutions of the final 3D reconstruction models were determined using a Fourier Shell Correlation (FSC) cut-off of 0.5 (Figure S5), and the number of particles used for each 3D reconstruction is summarized in Table S2.

The crystal structures of BG505 SOSIP.664 (PDB 3J5M), BG505 SOSIP.664 with PGV04 (PDB 3J5M), and 2G12 Fab (PDB 1OP5) were manually fitted into the EM densities and refined using the UCSF Chimera (Pettersen et al., 2004) 'Fit in map' function.

Additional details regarding electron microscopy, data processing, and image reconstruction can be found in Supplemental Experimental Procedures.

Supplementary Material

Refer to Web version on PubMed Central for supplementary material.

Acknowledgements

We thank John Mascola, Marshall Posner, James Robinson, and Dennis Burton for providing monoclonal antibodies, Pascal Poignard and Alejandra Ramos for providing BG505 gp120 and Richard Wilson for providing JRFL gp140-foldon. This study was supported by funding from the NIH HIVRAD (AI104722), the Scripps CHAVI-ID (AI100663) and IAVI, which is made possible by the support of many donors, including: the Bill & Melinda Gates Foundation, the Ministry of Foreign Affairs of Denmark, Irish Aid, the Ministry of Finance of Japan, the Ministry of Foreign Affairs of the Netherlands, the Norwegian Agency for Development Cooperation (NORAD), the United Kingdom Department for International Development (DFID), and the United States Agency for International Development (USAID). The full list of IAVI donors is available at http://www.iavi.org. This study is made possible by the generous support of the Bill & Melinda Gates Foundation Collaboration for AIDS Vaccine Discovery and the American people through USAID. The contents of this manuscript are the responsibility of IAVI and do not necessarily reflect the views of USAID or the US Government.

References

Binley JM, Sanders RW, Clas B, Schuelke N, Master A, Guo Y, Kajumo F, Anselma DJ, Maddon PJ, Olson WC, et al. A recombinant human immunodeficiency virus type 1 envelope glycoprotein complex stabilized by an intermolecular disulfide bond between the gp120 and gp41 subunits is an antigenic mimic of the trimeric virion- associated structure. J. Virol. 2000; 74:627–643. [PubMed: 10623724]

Blattner C, Lee JH, Sliepen K, Derking R, Falkowska E, de la Pena AT, Cupo A, Julien JP, van Gils M, Lee PS, et al. Structural delineation of a quaternary, cleavage-dependent epitope at the gp41-gp120 interface on intact HIV-1 Env trimers. Immunity. 2014; 40:669–680. [PubMed: 24768348]

Doria-Rose NA, Schramm CA, Gorman J, Moore PL, Bhiman JN, DeKosky BJ, Ernandes MJ, Georgiev IS, Kim HJ, Pancera M, et al. Developmental pathway for potent V1V2-directed HIV-neutralizing antibodies. Nature. 2014; 509:55–62. [PubMed: 24590074]

Falkowska E, Le KM, Ramos A, Doores KJ, Lee JH, Blattner C, Ramirez A, Derking R, van Gils MJ, Liang CH, et al. Broadly neutralizing HIV antibodies define a glycan-dependent epitope on the prefusion conformation of gp41 on cleaved envelope trimers. Immunity. 2014; 40:657–668. [PubMed: 24768347]

Forsell MN, Schief WR, Wyatt RT. Immunogenicity of HIV-1 envelope glycoprotein oligomers. Curr. Opin. HIV AIDS. 2009; 4:380–387. [PubMed: 20048701]

Guenaga J, de Val N, Tran K, Feng Y, Satchwell K, Ward AB, Wyatt RT. Well-Ordered Trimeric HIV-1 Subtype B and C Soluble Spike Mimetics Generated by Negative Selection Display Native-like Properties. PLoS Path. 2015; 11:e1004570.

Herrera C, Klasse PJ, Michael E, Kake S, Barnes K, Kibler CW, Campbell-Gardener L, Si Z, Sodroski J, Moore JP, et al. The impact of envelope glycoprotein cleavage on the antigenicity, infectivity, and neutralization sensitivity of Env-pseudotyped human immunodeficiency virus type 1 particles. Virology. 2005; 338:154–172. [PubMed: 15932765]

Huang J, Kang BH, Pancera M, Lee JH, Tong T, Feng Y, Georgiev IS, Chuang GY, Druz A, Doria-Rose NA, et al. Broad and potent HIV-1 neutralization by a human antibody that binds the gp41-gp120 interface. Nature. 2014; 515:138–142. [PubMed: 25186731]

Julien JP, Cupo A, Sok D, Stanfield RL, Lyumkis D, Deller MC, Klasse PJ, Burton DR, Sanders RW, Moore JP, et al. Crystal structure of a soluble cleaved HIV-1 envelope trimer. Science. 2013; 342:1477–1483. [PubMed: 24179159]

Khayat R, Lee JH, Julien JP, Cupo A, Klasse PJ, Sanders RW, Moore JP, Wilson IA, Ward AB. Structural characterization of cleaved, soluble HIV-1 envelope glycoprotein trimers. J. Virol. 2013; 87:9865–9872. [PubMed: 23824817]

Kong L, Lee JH, Doores KJ, Murin CD, Julien JP, McBride R, Liu Y, Marozsan A, Cupo A, Klasse PJ, et al. Supersite of immune vulnerability on the glycosylated face of HIV-1 envelope glycoprotein gp120. Nat. Struct. Mol. Biol. 2013; 20:796–803. [PubMed: 23708606]

Li Y, O'Dell S, Walker LM, Wu X, Guenaga J, Feng Y, Schmidt SD, McKee K, Louder MK, Ledgerwood JE, et al. Mechanism of neutralization by the broadly neutralizing HIV-1 monoclonal antibody VRC01. J. Virol. 2011; 85:8954–8967. [PubMed: 21715490]

Ludtke SJ, Baldwin PR, Chiu W. EMAN: semiautomated software for high-resolution single-particle reconstructions. J. Struct. Biol. 1999; 128:82–97. [PubMed: 10600563]

Lyumkis D, Julien JP, de Val N, Cupo A, Potter CS, Klasse PJ, Burton DR, Sanders RW, Moore JP, Carragher B, et al. Cryo-EM structure of a fully glycosylated soluble cleaved HIV-1 envelope trimer. Science. 2013; 342:1484–1490. [PubMed: 24179160]

McCune JM, Rabin LB, Feinberg MB, Lieberman M, Kosek JC, Reyes GR, Weissman IL. Endoproteolytic cleavage of gp160 is required for the activation of human immunodeficiency virus. Cell. 1988; 53:55–67. [PubMed: 2450679]

McLellan JS, Chen M, Joyce MG, Sastry M, Stewart-Jones GB, Yang Y, Zhang B, Chen L, Srivatsan S, Zheng A, et al. Structure-based design of a fusion glycoprotein vaccine for respiratory syncytial virus. Science. 2013; 342:592–598. [PubMed: 24179220]

Murin CD, Julien JP, Sok D, Stanfield RL, Khayat R, Cupo A, Moore JP, Burton DR, Wilson IA, Ward AB. Structure of 2G12 Fab2 in complex with soluble and fully glycosylated HIV-1 Env by negative-stain single-particle electron microscopy. J. Virol. 2014; 88:10177–10188. [PubMed: 24965454]

Pancera M, Wyatt R. Selective recognition of oligomeric HIV-1 primary isolate envelope glycoproteins by potently neutralizing ligands requires efficient precursor cleavage. Virology. 2005; 332:145–156. [PubMed: 15661147]

Pancera M, Zhou T, Druz A, Georgiev IS, Soto C, Gorman J, Huang J, Acharya P, Chuang GY, Ofek G, et al. Structure and immune recognition of trimeric pre-fusion HIV-1 Env. Nature. 2014; 514:455–461. [PubMed: 25296255]

Pettersen EF, Goddard TD, Huang CC, Couch GS, Greenblatt DM, Meng EC, Ferrin TE. UCSF Chimera--a visualization system for exploratory research and analysis. J. Comput. Chem. 2004; 25:1605–1612. [PubMed: 15264254]

Ringe RP, Sanders RW, Yasmeen A, Kim HJ, Lee JH, Cupo A, Korzun J, Derking R, van Montfort T, Julien JP, et al. Cleavage strongly influences whether soluble HIV-1 envelope glycoprotein trimers adopt a native-like conformation. Proc. Natl. Acad. Sci. U.S.A. 2013; 110:18256–18261. [PubMed: 24145402]

Sanders RW, Derking R, Cupo A, Julien JP, Yasmeen A, de Val N, Kim HJ, Blattner C, de la Pena AT, Korzun J, et al. A next-generation cleaved, soluble HIV-1 Env Trimer, BG505 SOSIP.664 gp140, expresses multiple epitopes for broadly neutralizing but not non-neutralizing antibodies. PLoS Path. 2013; 9:e1003618.

Sanders RW, Vesanen M, Schuelke N, Master A, Schiffner L, Kalyanaraman R, Paluch M, Berkhout B, Maddon PJ, Olson WC, et al. Stabilization of the soluble, cleaved, trimeric form of the envelope glycoprotein complex of human immunodeficiency virus type 1. J. Virol. 2002; 76:8875–8889. [PubMed: 12163607]

Scharf L, Scheid JF, Lee JH, West AP Jr. Chen C, Gao H, Gnanapragasam PN, Mares R, Seaman MS, Ward AB, et al. Antibody 8ANC195 reveals a site of broad vulnerability on the HIV-1 envelope spike. Cell Rep. 2014; 7:785–795. [PubMed: 24767986]

Sok D, van Gils MJ, Pauthner M, Julien JP, Saye-Francisco KL, Hsueh J, Briney B, Lee JH, Le KM, Lee PS, et al. Recombinant HIV envelope trimer selects for quaternary-dependent antibodies targeting the trimer apex. Proc. Natl. Acad. Sci. U.S.A. 2014; 111:17624–17629. [PubMed: 25422458]

Stamatatos L, Morris L, Burton DR, Mascola JR. Neutralizing antibodies generated during natural HIV-1 infection: good news for an HIV-1 vaccine? Nat Med. 2009; 15:866–870. [PubMed: 19525964]

Tran K, Poulsen C, Guenaga J, de Val N, Wilson R, Sundling C, Li Y, Stanfield RL, Wilson IA, Ward AB, et al. Vaccine-elicited primate antibodies use a distinct approach to the HIV-1 primary receptor binding site informing vaccine redesign. Proc. Natl. Acad. Sci. U.S.A. 2014; 111:E738–747. [PubMed: 24550318]

West AP Jr. Scharf L, Scheid JF, Klein F, Bjorkman PJ, Nussenzweig MC. Structural insights on the role of antibodies in HIV-1 vaccine and therapy. Cell. 2014; 156:633–648. [PubMed: 24529371]

Wu X, Yang ZY, Li Y, Hogerkorp CM, Schief WR, Seaman MS, Zhou T, Schmidt SD, Wu L, Xu L, et al. Rational design of envelope identifies broadly neutralizing human monoclonal antibodies to HIV-1. Science. 2010; 329:856–861. [PubMed: 20616233]

Highlight Bullets

- HIV-1 soluble spike mimetics were generated by covalent linkage of the two subunits
- The native, flexibly linked (NFL) trimers do not require furin-mediated cleavage
- The NFL trimers are well-ordered as determined by biophysical analysis and EM
- The NFL platform is transferable to subtypes A, B, and C trimers

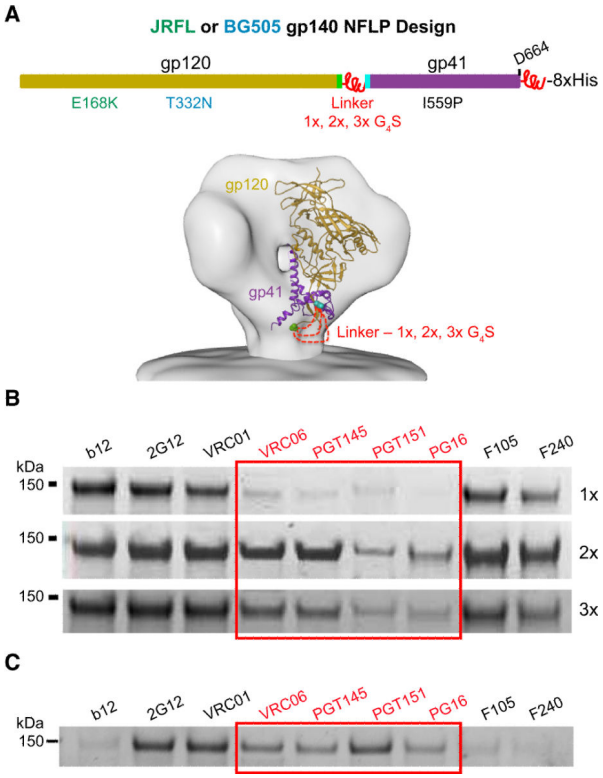

Figure 1. NFL trimer design and linker length screening

(A) Top, schematic representing the NFL trimer design. The NFL glycoprotein trimers contain an N-terminal CD5 leader sequence followed by gp120 covalently linked to gp41 by 1, 2 or 3 copies of G_4S flexible peptide linkers. The C-terminus of gp41 has one copy of the G_4S linker followed by a His_8 tag. Both proteins were designed with and without the I559P substitution. JRFL gp140 NFLs possess an additional substitution of E168K for PG9/PG16 recognition, while BG505 gp140 NFLs have a T332N mutation for the N332 glycan supersite. Bottom, model of gp120 (in golden rod with C-terminus in green) linked to gp41 (in purple with N-terminus in turquoise) by different linker lengths (red dashed lines) in the context of the viral spike; one protomer is shown for clarity. (B) JRFL gp140 NFLP with 1-3x G_4S linkers were screened by IP with selected mAbs, Trimer-specific bNAbs are highlighted in red. (C). IP of BG505 gp140 NFL2P from crude cell supernatant by selected mAbs (trimer-specific mAbs highlighted in red). Note that the IP band intensity for non-NAb F105 is relatively light compared to those of the bNAbs, suggesting the majority of expressed protein is well-ordered trimers. See also Figure S1.

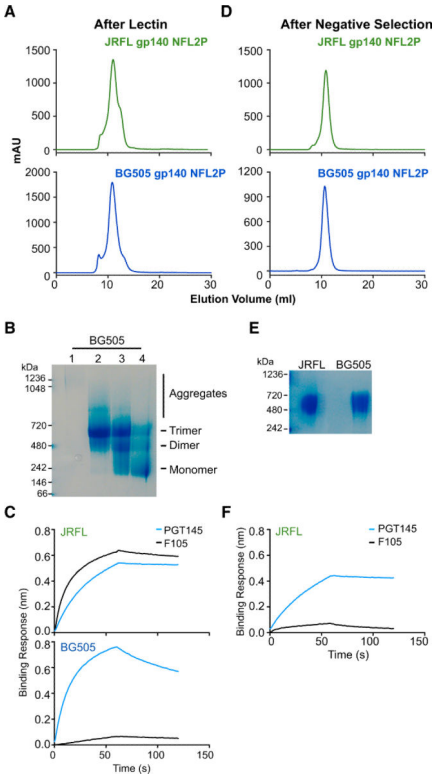

Figure 2. Purification of JRFL and BG505 gp140 NFL2P

(A). SEC profile of lectin purified JRFL (top) and BG505 (bottom) gp140 NFL2Ps. (B) Blue native gel analysis of select fractions from SEC of BG505 gp140 NFL2P. Lane 1) first peak, aggregates, 2) second peak, trimer, 3-4) third peak, dimer/monomer. (C) PGT145 and F105 binding profile of JRFL (top) and BG505 (bottom) gp140 NFL2P from SEC purified trimer peak by BLI. (D) SEC profile of JRFL (top) and BG505 (bottom) gp140 NFL2P after negative selection. (E) Blue native gel analysis of JRFL and BG505 gp140 NFL2P after negative selection. (F) PGT145 and F105 binding profile of JRFL gp140 NFL2P after negative selection. See also Figure S1C.

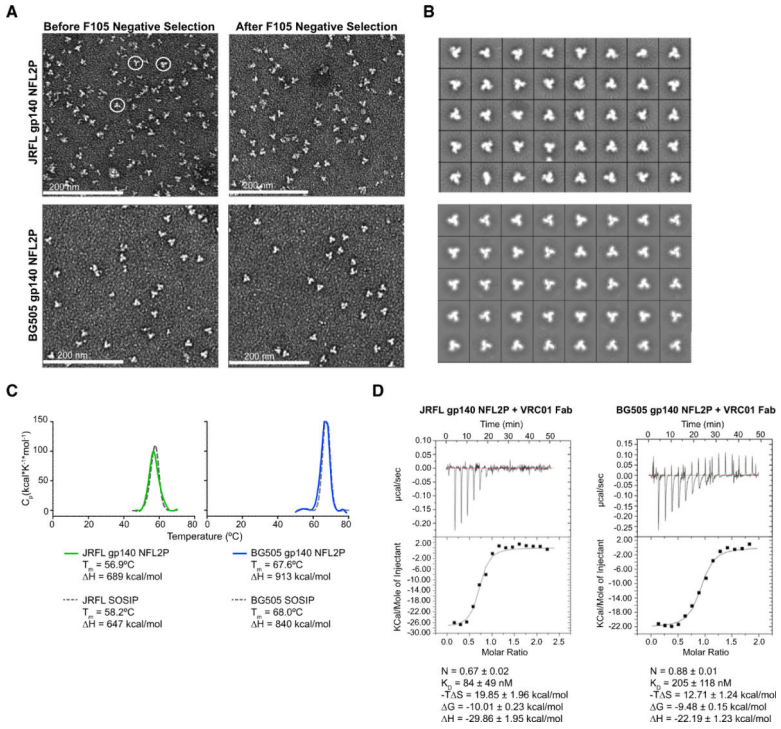

Figure 3. Negative stain EM analysis and thermal stability of purified JRFL and BG505 gp140 NFL2P trimers

(A) Negative stain EM micrographs of JRFL (top) and BG505 (bottom) gp140 NFL2P before (left) and after (right) negative selection. For JRFL, negative selection enriched for well-ordered trimers, whereas, no noticeable difference was observed for BG505 before and after negative selection. White scale bars, 200 nm. (B) 2D class averages of JRFL (top) and BG505 (bottom) gp140 NFL2P. (C) DSC melting profiles comparing JRFL (left) and BG505 (right) gp140 NFL2P trimers to respective SOSIP trimers. (D) The raw data (top) and binding isotherms (bottom) from ITC measuring the binding of JRFL (left) and BG505 (right) gp140 NFL2P to VRC01 Fab. See also Figure S2.

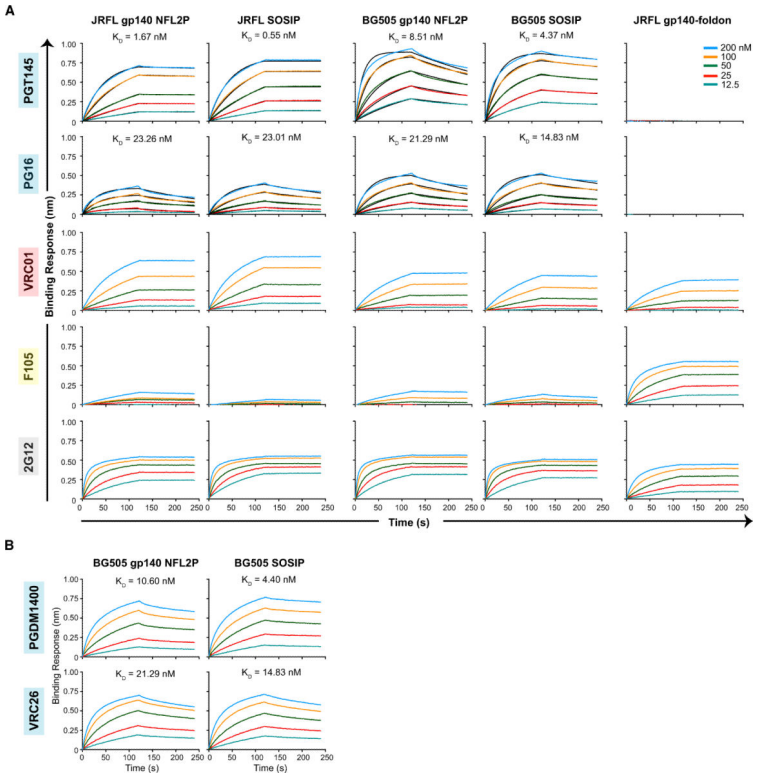

Figure 4. Antigenic profiles of JRFL and BG505 trimers by BLI

Anti-human Fc sensors were used to capture the mAbs and the trimers were used as an analyte at various concentrations (200-12.5 nM). The black curves for PG145 and PG16 in (A) and PGDM1400 and VRC26 in (B) depict theoretical Langmuir fits generated by 1:1 binding kinetics. Trimer-specific bNAbs (PGT145, PG16, PGDM1400, and VRC26); CD4bs-directed bNAb, VRC01; glycan-directed bNAb, 2G12; non-Nab, F105. See also Figure S3 and Table S1.

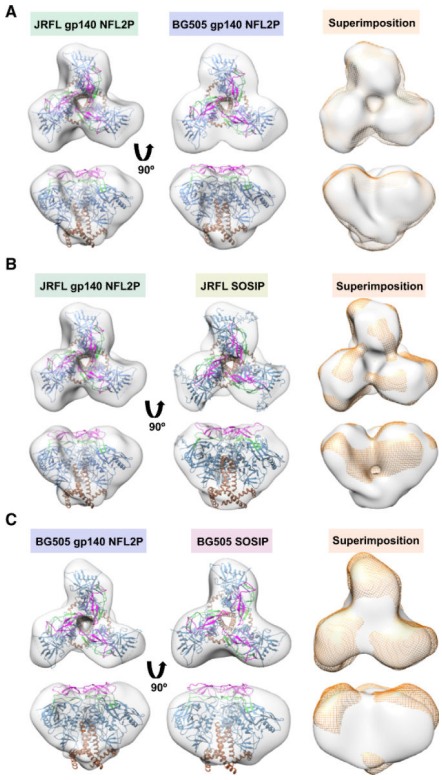

Figure 5. EM 3D reconstructions of unliganded JFRL and BG505 gp140 NFL2P compared with JRFL and BG505 SOSIP

(A) Top and side views of unliganded JRFL (left) and BG505 (middle) gp140 NFL2P 3D reconstruction EM densities in gray. The BG505 SOSIP crystal structure (PDB 3J5M) is fitted within (gp120 in blue, V1V2 in magenta, V3 in green and gp41 in brown). On the right, BG505 uncleaved trimer EM density (orange) is superimposed on the JRFL uncleaved trimer EM density (gray). (B) Top and side views of unliganded JRFL gp140 NFL2P and JRFL SOSIP in gray with BG505 SOSIP crystal structure fitted within as in (A). To the right, JRFL gp140 NFL2P EM density (orange) is superimposed on JRFL SOSIP EM density (gray). (C) Top and side views of unliganded BG505 gp140 NFL2P and BG505 SOSIP in gray with BG505 SOSIP crystal structure fitted within as above. On the right, BG505 gp140 NFL2P EM density (orange) is superimposed on BG505 SOSIP EM density (gray). See also Figures S4-5 and Table S2.

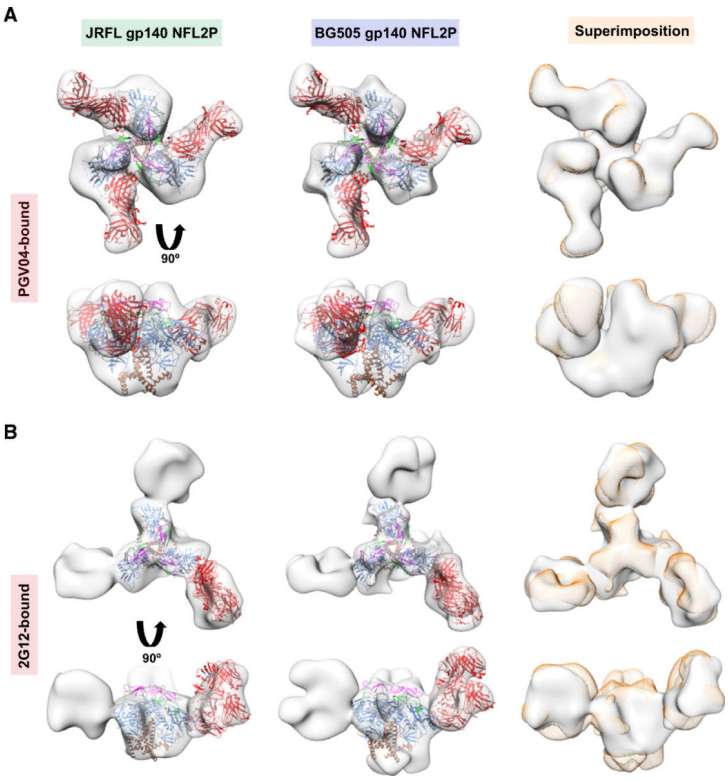

Figure 6. EM 3D reconstructions of PGV04-liganded and 2G12-liganded JRFL and BG505 gp140 NFL2P trimers

(A) Top and side views of the PGV04-liganded uncleaved trimers (in gray) with the PGV04-bound gp140 structure (PDB 3J5M; gp120 in blue, V1V2 in magenta, V3 in green, gp41 in brown and PGV04 in red) fitted within the EM density. (B) Top and side views of the 2G12-liganded uncleaved trimers with the 2G12-bound gp120 core crystal structure (PDB 1OP5; gp120 in blue, V1V2 in magenta, V3 in green, gp41 in brown and 2G12 in red) fitted in the EM density. On the right of each panel are top and side views of the BG505 uncleaved trimer EM density (in orange) superimposed on the JRFL uncleaved trimer EM density (in gray). See also Figures S4-5 and Table S2.

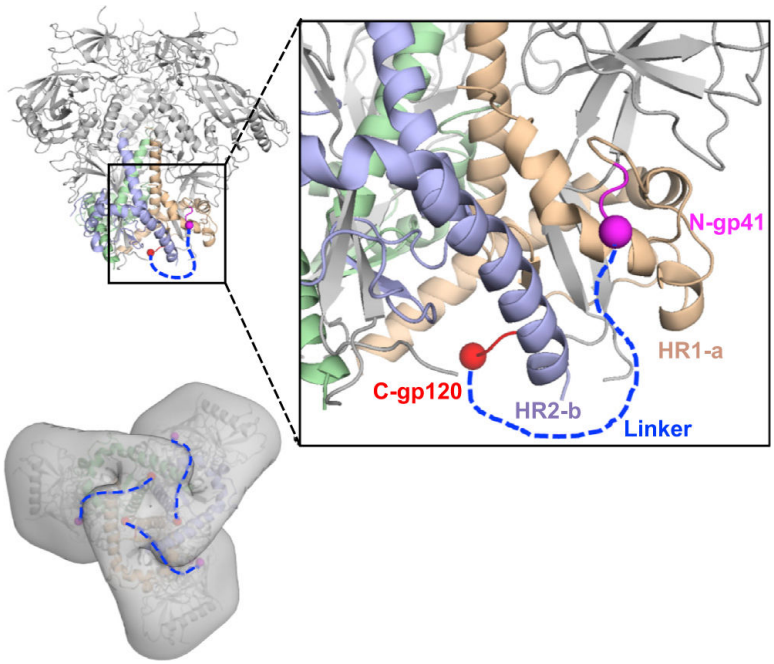

Figure 7. Model of the gp120-gp41 flexible linker using the BG505 SOSIP structure

Top left, high-resolution crystal structure of the PGT122- and 35O22-liganded BG505 SOSIP trimer (PDB 4TVP) with gp120 subunits colored in gray and gp41 subunits colored in green, violet and wheat, respectively (Fabs not shown for clarity). Top right, enlargement of the gp41-gp120 associated regions within the trimer. The blue dash line represents the flexible linker joining the last residue of the gp120 C-terminus (in red) to the first residue (visible in this structure) of the gp41 fusion peptide (in magenta). Bottom left, BG505 SOSIP crystal structure fitted within the EM density of the JRFL gp140 NFL2P trimer. Blue dotted lines represent the three flexible linkers on the surface EM contours, joining each of the three subunits that comprise the soluble NFL Env trimer.